Absorption of longitudinal ultrasound by superconducting indium and dilute alloys of tin in indium*

David E. Binnie, Robert W. Reed, and F. G. Brickwedde
Department of Physics, The Pennsylvania State University, University Park, Pennsylvania 16802
(Received 1 October 1973)

Measurements were made of the absorption of sound (20–180 MHz) in pure In and alloys of 0.01, 0.03, and 0.09-at.% Sn in In, in the superconducting and normal states between 1 and 4.2 K. When the absorption data were handled by the usual method, i.e., by using only experimental data between 1 K $< T < 0.85T_c$ and making Δ_0, and $\alpha'_n(1\text{ K})$ adjustable parameters to obtain the best fit of the BCS $\Delta(T)$ function to the experimental data, the Δ_0's obtained for pure In were in agreement with the Δ_0's for In determined by other observers using the ultrasonic technique. But all of these ultrasonic values for Δ_0 are low relative to Δ_0's determined by other experimental techniques. Extrapolating to 0 K, $\Delta(T)$'s calculated from the BCS relation, $\alpha'_s/\alpha'_n = 2f(\Delta/T)$, yielded $\Delta_0 = 1.85kT_c$ in agreement with Δ_0's determined by techniques other than ultrasonic, but the calculated $\Delta(T)$'s deviated considerably from the BCS function for $\Delta(T)$. The departure from the BCS equation of our calculated $\Delta(T)$'s, and the disagreement of the ultrasonic Δ_0's with other Δ_0's are attributed to sonic absorption by line dislocations set in vibration by the sound and damped by the conduction electrons. It was established experimentally that for our specimens and apparatus, the dislocation attenuation was independent of the sonic amplitude. Our experimental $\alpha'_s(T)$, $\alpha'_n(T)$ data were analyzed using the theory of Mason for attenuation by dislocations independent of the sonic amplitude and the BCS theory. The results of this analysis are consistent with both theories and with data obtained using other than ultrasonic techniques.

I. INTRODUCTION

This research was undertaken to investigate the crystalline anisotropy of the superconducting energy-gap parameter $\Delta_0 \equiv \Delta(T=0)$ in In, using the ultrasonic-absorption technique, in particular for a study of the dependence of the anisotropy on the electron mean free path l. The electron free path was varied by alloying with 0.01, 0.03, and 0.09-at.% Sn. As the research progressed, it became an investigation of ultrasonic absorption in In by line dislocations (lattice defects). Absorption by the dislocations occurs along with the direct absorption of sonic energy by the conduction electrons. Ultrasonic absorption by line dislocations in soft metals is usually considered to be dependent on the sonic amplitude. However, the absorption which we observed and attributed to line dislocations is independent of the sonic amplitude and fits Mason's[1] theory for amplitude-independent absorption by line dislocations.

The coefficients α_s and α_n for the absorption of longitudinal sound by conduction electrons in the superconducting and normal states are related to the energy-gap parameter $\Delta(T)$ by the BCS equation[2]

$$\frac{\alpha_s(T)}{\alpha_n(T)} = 2\left[1 + e^{\Delta(T)/kT}\right]^{-1} \equiv 2f(\Delta(T)/kT)\ . \qquad (1)$$

The BCS theory gives the dependence of $\Delta(T)/\Delta_0$ on $t = T/T_c$ in integral form. There is not a closed analytic expression for $\Delta(t)/\Delta_0$. Mühlschlegel[3] has tabulated it. For it, we have used the following approximate expression from Bliss and Rayne,[4] accurate to 0.05%:

$$\Delta(t)/\Delta_0 = [\cos(\tfrac{1}{2}\pi t^2)]^{1/2} - 1.15\times10^{-3}\, e^{3.8t} \times \sin[5.46(1-t)]\ . \qquad (2)$$

Values of Δ_0 have been derived from experimental α'_s, α'_n data by two methods: (i) by the method of least squares, finding the value of Δ_0 that yields the best fit of the experimental α'_s, α'_n data to the BCS relations (1) and (2), and (ii) by graphical extrapolation to 0 K of the $\Delta(T)$'s calculated from the experimental data using Eq. (1).

Table I summarizes previous determinations of Δ_0 for pure In. There are two things about the Table I data that are important here:

(a) The value $\Delta_0 = 1.83kT_c$, obtained from precise, critical magnetic field H_c data by Finnemore and Mapother[5] is probably the best value we have for Δ_0 when averaged over all crystal orientations. According to Anderson's theory[6] for "dirty" superconductors, it is the value to be expected for Δ_0 when $l \ll \xi_0$ (the coherence length in pure metal), wiping out the crystalline anisotropy of Δ_0. We find $\Delta_0 = (1.85 \pm 0.05)kT_c$ for our 0.09-at.%-Sn–In alloy.

(b) The ultrasonically determined values for Δ_0, while in good agreement with each other are the lowest in Table I. Their range is outside the range of Δ_0 determined using other techniques. Table I gives no clear evidence for anisotropy in Δ_0.

We find that $\Delta(T)$'s calculated from our $\alpha'_s(T)$,

TABLE I. Summary of determinations of the energy-gap parameter Δ_0/kT_c.

	No. of investigations	Range
Optical: transmission and reflection[a,b,c]	3	1.9_5–2.2
Tunneling[d,e,f,g]	4	1.7–1.85
Specific heat[h]	1	1.6–1.9
Critical magnetic field[i]	1	1.82–1.84
Ultrasonic attenuation (longitudinal sound, fct crystal)[j,k,l] direction of $\vec{q}$:		
[100]	3	1.59–1.72
[001]	3	1.52–1.57
[110]	3	1.55–1.70

[a]See Ref. 7. [e]See Ref. 11. [i]See Ref. 5.
[b]See Ref. 8. [f]See Ref. 12. [j]See Ref. 15.
[c]See Ref. 9. [g]See Ref. 13. [k]See Ref. 16.
[d]See Ref. 10. [h]See Ref. 14. [l]See Ref. 17.

$\alpha_n'(T)$ data for pure In and two of the three alloys (0.01 and 0.03 at.%) using Eq. (1) depart significantly from the BCS $\Delta(T)$ relation, Eq. (2). We attribute this and the low Δ_0's by the ultrasonic technique to absorption of sonic energy by line dislocations.

II. EXPERIMENTAL

The single crystals of pure In and of In alloyed with Sn used in this study were supplied by Research Crystals, Inc., Richmond, Virginia, and were grown by the Czochralski method, starting with 99.9999%-pure In and Sn. The Sn content of the alloyed crystals was verified by Ledroux and Company, Teaneck, New Jersey. The Sn content of the alloys was 0.01 ± 0.005, 0.03 ± 0.01, and 0.09 ± 0.01 at.%.

The resistance ratio, $\rho_{300}/\rho_{4.2}$, was measured using the eddy-current-decay method.[18] The resistance ratios were 8950 ± 450 for pure In, and 925 ± 45, 562 ± 30, and 250 ± 18 for the alloys in order of increasing Sn concentrations.

A "Servomet *SMD*" spark cutting machine was used to cut specimens in the form of right circular cylinders (~1 cm in diameter and 0.7 cm long) from the large single crystals. All of the spark cutting and spark planing was done at the lowest speeds in order to minimize damage to the crystal. Specimens with cylinder axes along the [100], [001], and [110] directions in the fct lattice were cut from each of the single crystals. Specimens were bonded to a lithium-niobate 20-MHz transducer with low-temperature epoxy.

Acoustic measurements were made with the specimens in contact with the liquid-He bath. The specimen temperature was measured with a four-lead Ge resistance thermometer, calibrated from 1.5 to 4.2 K by Cryocal, Inc. The calibration was extended to 0.8 K by comparison with a second Ge resistance thermometer calibrated from 0.75 to 4.2 K by Professor Gaines, Department of Physics, Ohio State University for Lake Shore Cryotronics, Inc. The calibration was checked by ourselves against the 1958 He^4 Vapor-Pressure Scale of Temperature[19] at temperatures above 1.2 K. The calibration is believed accurate to better than ± 0.01 K. The thermometer current, 1.203 μA, was provided by a constant-current supply stable to better than 0.01%. The potential difference across the thermometer was amplified with a Hewlett-Packard Model No. 740B differential voltmeter and was recorded on the x axis of an X-Y recorder. On the Y axis was recorded the amplitude of the acoustic echo from a pure In or an In alloy specimen.

The ultrasonic attenuation was measured using the pulse-echo method with a single transducer which served as both the sonic driver and receiver. The frequencies used were the odd harmonics of 20 up to 180 MHz. The ultrasonic apparatus which has been described elsewhere[20] incorporated features which allowed operation at very low sonic amplitudes without the sacrifice of long-term stability necessary for continuous recording of the amplitude of a sonic echo. Major features of the ultrasonic system were as follows: (i) The receiver was stabilized by an automatic gain control. (ii) A *low noise* rf preamplifier was used at the front end of the receiver for improved signal-to-noise ratio. (iii) A gated integrating amplifier was used to select a single echo and have a dc output voltage proportional to the amplitude of the echo. (iv) The scale on which echo voltages were recorded at the recorder was calibrated in dB with calibrated attenuators in the transmitting line between the transducer and the driving rf pulsed oscillator. (v) The attenuators were accurate to ± 0.2 dB. (vi) The rf driving pulses to the transducer were 1–2 μsec wide, had a repetition rate of 1000 Hz, and were 10 mW or less at the transducer.

Changes in the amplitude of an echo were recorded continuously for temperature sweeps, up and down, over the range 1–4.2 K. Several sweeps were recorded for different ultrasonic frequencies and echo numbers and for the different specimens varying in composition and crystalline orientation. As the liquid-He cryostat was pumped and the temperature drifted below T_c, the amplitude of the receiver signal at the X-Y recorder increased and approached the limit of the Y scale. The dynamic range of the Y scale was 15 dB. In order to keep the recorder pen within the 15-dB dynamic range (see Fig. 1), 10 dB of additional attenuation was switched into the transmission line between the

TABLE II. Results of calculations by method I of Δ_0 and $\alpha_n(0)$ from the experimental data of this investigation.

Purity	Direction of $\vec{q}$	Frequency (MHz)	No. of charts	Δ_0/kT_c	$\alpha_n(0)$ (calc. from best fit of data) (dB/cm)	$\alpha_n'(0)$ (expt) (dB/cm)	$\frac{\alpha_n(0)\ (\text{calc})}{\alpha_n'(0)\ (\text{expt})}$	ql
Pure In	[001]	20	6	1.46 ± 0.05	1.81	3.12	0.58	2.5
		60	4	1.49 ± 0.03	10.0	14.9	0.67	7.6
	[100]	20	6	1.58 ± 0.05	2.42	3.78	0.64	2.5
		60	4	1.61 ± 0.05	9.37	13.4	0.70	7.4
	[110]	20	4	1.52 ± 0.04	3.18	6.79	0.47	2.3
		60	3	1.46 ± 0.03	15.0	22.9	0.65	6.8
In–0.01-at.% Sn	[001]	60	2	1.72 ± 0.03	7.47	9.07	0.82	0.79
		100	4	1.73 ± 0.02	14.9	17.1	0.87	1.3
		140	4	1.76 ± 0.04	22.5	24.6	0.91	1.8
	[100]	60	2	1.67 ± 0.01	5.52	7.52	0.73	0.77
		100	4	1.73 ± 0.02	12.2	14.4	0.84	1.3
	[110]	60	2	1.78 ± 0.02	9.11	11.3	0.80	0.71
		100	4	1.73 ± 0.02	19.3	24.9	0.78	1.2
In–0.03-at.% Sn	[001]	100	4	1.82 ± 0.03	10.0	11.0	0.91	0.80
		140	3	1.76 ± 0.01	17.1	20.3	0.84	1.1
	[100]	100	6	1.78 ± 0.03	8.75	10.1	0.87	0.78
		140	4	1.77 ± 0.02	14.6	16.1	0.91	1.1
	[110]	100	6	1.74 ± 0.05	11.0	13.5	0.82	0.72
		140	6	1.79 ± 0.05	19.5	23.4	0.84	1.0
In–0.09-at.% Sn	[001]	60	4	1.82 ± 0.04	0.96	1.24	0.78	0.22
		100	4	1.83 ± 0.05	3.58	3.83	0.93	0.39
		140	4	1.87 ± 0.03	7.28	7.46	0.97	0.54
		180	3	1.80 ± 0.04	10.6	12.0	0.89	0.69
	[100]	140	4	1.76 ± 0.07	5.57	6.09	0.91	0.52
		180	3	1.89 ± 0.04	10.0	10.4	0.97	0.69
	[110]	140	7	1.85 ± 0.08	8.03	8.67	0.93	0.50
		180	2	1.96 ± 0.02	13.4	13.6	0.98	0.63

pulsed oscillator and the transducer. Figure 1 is a typical recorder chart. The Y axis of each chart was calibrated in dB at the lowest temperature reached in that run.

Amplitude-dependent attenuation was minimized. Tests at low sonic powers (0.3 to 30 mW from transmitter to transducer) showed there was no apparent amplitude-dependent attenuation. Thus (a) The dB calibrations of our X-Y recorder charts at 1 K and above T_c (for a 20 dB difference in sonic power) agreed to within ± 0.1 dB; (b) the ratio $(\alpha_n - \alpha_s)/(\text{echo number})$ was independent of echo number and was constant over a 20-dB range; (c) insertion of 10 dB of attenuation in the electrical transmission line before the sonic specimen produced the same change in receiver output at the recorder as 10 dB inserted in the receiver line after the specimen. An increase of sonic power by 30–40 dB (10–100 W to the transducer) did produce amplitude-dependent absorption.

Attenuation in the normal state α_n was measured with a magnetic field in excess of 280 Oe imposed on the specimen to destroy its superconductivity. This field was generated with an iron cored electromagnet on the outside of the liquid-He cryostat. The magnet was rolled away for measurements in the superconducting state. Absorption in the normal state of specimens with 0.03 and 0.09 at.% Sn was independent of T below T_c. The 0.01 at.% specimen had a temperature-dependent α_n, and pure In exhibited magnetoacoustic oscillations in α_n which made a precise determination of α_n for pure indium less reliable. Hence, there is an uncertainty in α_n for pure In of ± 0.4 dB; $\alpha_n'(0)$ was ~ 20 dB.

III. INTERPRETATION OF EXPERIMENTAL DATA

Experimental values for the sonic absorption coefficients were obtained from the X-Y recorder charts. They are distinguished from calculated or otherwise deduced values by the prime superscript which appears on the experimental values. α and α' characterize absorption attributable, directly and indirectly, to the conduction electrons. $\alpha_s'(0)$ and $\alpha_s(0)$, characterizing the superconducting state at 0 K, are assumed to be zero. $\alpha_n'(0)$ and $\alpha_n(0)$ are coefficients for absorption in the normal state at 0 K; they are measures in dB of the difference in the amplitudes on the X-Y graph of a sonic echo from a specimen in the normal and in the superconducting states at 0 K. At other temperatures, $\alpha_s'(T)$ and $\alpha_n'(T)$ are the differences measured in

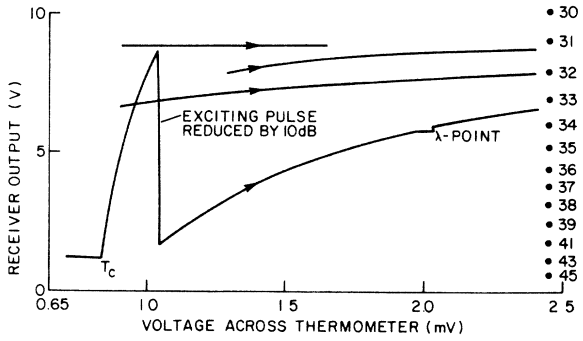

FIG. 1. Receiver output (echo signal amplitude) vs thermometer voltage. Thermometer scale factor (mV/cm) for curves 1 and 2 is indicated by the bottom scale. For curves 3 and 4, multiply by 5 the thermometer scale factor for curves 1 and 2. Points at right-hand side are receiver calibration points with nominal attenuator settings given in dB.

dB between the amplitudes of the echo pulse in the superconducting and normal states, respectively, at T and the amplitude of the same echo in the superconducting state at 0 K. The echo-amplitude data for the superconducting state were extrapolated from 1 down to 0 K in order to obtain the fiducial zero ordinate for all $\alpha'(T)$'s. $\alpha_s'(T_c) = \alpha_n'(T_c)$.

Echo-amplitude and thermometer voltage data were read from the X-Y charts to the nearest 0.1 mm and were converted to $\alpha'(T)$ data using an electronic computer and a three-point method of interpolation. The $\alpha'(T)$'s were determined at 0.1-K intervals from 1 to 4.2 K.

Δ_0's were derived from the experimental $\alpha_s'(T)$, $\alpha_n'(T)$ data by methods referred to here as methods I and II.

Method I

Method I for calculating Δ_0 utilized an analytical "curve-fitting" procedure. Δ_0 and $\alpha_n(0)$ were regarded as undetermined parameters to be determined by finding values for Δ_0 and $\alpha_n(0)$ that yielded the best fit of the experimental $\alpha_s'(T)$ data with the $\alpha_s(T)$ values calculated using Eqs. (1) and (2) and the trial values of Δ_0 and $\alpha_n(0)$. The best fit minimized $\sum[\alpha_s'(T) - \alpha_s(T)]^2$, where the sum extended from $T = 1$ K to $0.85T_c = 2.9$ K. Experimental data in the range $0.85T_c < T < T_c$ were not included and $\alpha_n(0)$ was made adjustable in keeping with a commonly made assumption[21] that in addition to the normal electronic absorption of the lorgitudinal sound there occurs other electronic absorption of nonlongitudinal sound, generally assumed to be transverse sound, which is practically completely damped out in the superconduction state in a small-ΔT range below T_c. In the calculation, $\alpha_n(T)$ was set equal to $[\alpha_n(0)/\alpha_n'(0)]\,\alpha_n'(T)$. This curve-fitting method for getting Δ_0 from ultrasonic-absorption data was used by Sinclair[15] whose Δ_0 values are included in Tables I and III.

The results of this curve-fitting procedure are given in Table II. The electron mean free paths l in Table II were calculated using the equation

$$l = \frac{\hbar}{\rho e^2}\left(\frac{3\pi^2}{n^2}\right)^{1/3} , \tag{3}$$

where ρ is the resistivity, e is the electronic charge, and n is the number density of conduction electrons (three per In atom). The ρ's at 4.2 K for the different specimens were calculated from their measured resistance ratios, $R_{300}/R_{4.2}$. The mean free paths at liquid-He temperatures were 5.5×10^{-4}, 2.2×10^{-4}, and 1.5×10^{-4} cm for the 0.01, 0.03, and 0.09 at.% Sn alloys, respectively, and 55×10^{-4} cm for the pure-In specimen. The Table II values for Δ_0 for pure In are averaged in Table III for each of the three crystalline orientations of $\vec{q}$. Table III compares our values for Δ_0 for pure In with the values of Δ_0 determined ultrasonically by other observers. The ± numbers by the Δ_0 values are assigned by the different investigators and represent only the scattering of the data.

Table III compares our experimental pure-In values for $\alpha_n'(0)/f$ for large values of ql with values of other observers. Here, f is the sonic frequency. The free-electron values of $\alpha_n(T)/f$ in Table III were calculated using[22]

$$\alpha_n/f = \pi^2 n m v_F/3DV_s^2 , \tag{4}$$

where n is the number density of conduction elec-

TABLE III. Comparison of Δ_0 (calculated by method I) and experimental $\alpha_n'(0)$ data for pure In with data of other observers using the ultrasonic technique.

Direction of $\vec{q}$	Values of Δ_0/kT_c				Large ql values (expt) of $\alpha_n'(0)/f$ (dB/cm MHz)					
	Present work	S[a]	FL[b]	FSB[c]	Present work	S[a]	FL[b]	FSB[c]	BR[d]	FE[e]
[001]	1.47 ± 0.05	1.52	1.55 ± 0.10	1.57 ± 0.05	0.25	0.27	0.24	0.19	0.27	0.52
[100]	1.60 ± 0.05	1.59	1.60 ± 0.10	1.72 ± 0.05	0.22	0.26	0.22	0.16	0.23	0.50
[110]	1.49 ± 0.05	1.70	1.55 ± 0.10	1.67 ± 0.05	0.38	0.39	0.36	0.33	0.40	0.43

[a] A. C. E. Sinclair, Ref. 15.
[b] K. Fossheim and J. R. Leibowitz, Ref. 16.
[c] V. D. Fil, O. A. Shevchenko, and P. A. Bezuglyi, Ref. 17.
[d] E. S. Bliss and J. A. Rayne, Ref. 4.
[e] Free-electron calculation taken from Bliss and Rayne, Ref. 4.

trons, D is the mass density of In, m is the electron mass, v_F is the Fermi velocity, and V_s is the sound speed.

Our Table III values for Δ_0 for pure In and the three alloys are represented in Fig. 2 by the solid black symbols.

The following conclusions were drawn from the results in Tables II and III and Fig. 2, based on the use of method I.

(a) Our values for Δ_0 for pure single-crystal In agree with the previously determined ultrasonic values to within the uncertainties of the experimental measurements, the uncertainties of which are larger than the scattering of the experimental data given by the ± figures in Table III. These ultrasonic values for Δ_0 are low when compared with the BCS value of $1.76kT_c$ and low when compared with the values in Table I determined by other methods; in particular they are low when compared with the Finnemore and Mapother value of $1.83kT_c$.

(b) Δ_0 increases with the Sn concentration in the alloy specimens and approaches $1.85kT_c$ at 0.09-at.% Sn which agrees with the Finnemore and Mapother value of $1.83kT_c$ within our experimental uncertainty.

(c) If there is crystalline anisotropy of Δ_0 in In, it is by method I smaller than $\pm 0.1kT_c$, the estimated over-all uncertainty of our Δ_0 values.

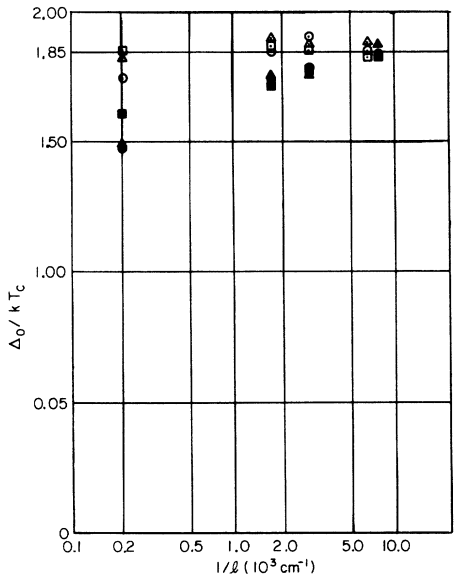

FIG. 2. Comparison of Δ_0/kT_c determined using the experimental $\alpha_s'(T)$, $\alpha_n'(T)$ data with method I (solid symbols) and method II (open symbols). Symbols: squares, for $\vec{q}$ in [100] direction; circles, in the [001] direction; and triangles, in the [110] direction. l is the electron mean free path. Specimens: pure In and three alloys (0.01, 0.03, and 0.09-at.% Sn).

Method II

Method II consisted of a *graphical* extrapolation to 0 K of the $\Delta(T)$'s calculated from the experimental $\alpha_s'(T)$, $\alpha_n'(T)$ data using Eq. (1). A $\Delta(T)$-vs-T plot was made for each X-Y recorder chart, a value of $\Delta(T)$ being calculated for each selected point of the chart at 0.1 K intervals. Each $\Delta(T)$-vs-T plot was extrapolated to 0 K yielding a value of Δ_0. Method II differed from method I in that (i) method II made no use of Eq. (2) whereas Eq. (2) was essential to method I, and (ii) whereas $\alpha_n(0)$ was an adjustable parameter in method I determined by minimizing the sum of the squared deviations, in method II the experimental values of $\alpha_n'(T)$ were used.

For each X-Y recorder chart, $\Delta(T)$'s were calculated for different assumed values of $\alpha_s'(1\text{ K})$ which were approximately 0.1 dB. The ends of the $\Delta(T)$-vs-T graphs near 0 K are very sensitive to small changes in $\alpha_s'(1\text{ K})$; an increase in $\alpha_s'(1\text{ K})$ swings the end of the $\Delta(T)$ curve down, whereas a decrease in $\alpha_s'(1\text{ K})$ swings it up. The value adopted for $\alpha_s'(1\text{ K})$ yielded a smooth extrapolation of $\Delta(T)$ to 0 K and made $[d\Delta(T)/dT]_{0\text{ K}} = 0$.

The values of Δ_0 obtained by extrapolation to 0 K were averaged for all X-Y recorder charts for one orientation of $\vec{q}$. These averages for different orientations of $\vec{q}$ and for different concentrations of Sn are represented in Fig. 2 by the open symbols.

The shapes of the $\Delta(T)$-vs-T graphs, except for the 0.09-at.%-Sn specimens, differed significantly from that predicted by the BCS theory, Eq. (2). Typical graphs for pure-In and 0.09-at.%-Sn specimens are shown in Fig. 3. The graph of the BCS Eq. (2) for $\Delta_0 = 1.85kT_c$ is included for comparison. See also the $\Delta(T)$ data from method II in Figs. 6 and 7 where they are represented by the ×'s.

The following conclusions were drawn from our method II results (see Figs. 2 and 3).

(i) Our $\alpha_s'(T)$, $\alpha_n'(T)$ data with method II yield $(1.85 \pm 0.10)kT_c$ for Δ_0 for pure In and for the three Sn alloys, independent of their Sn content or electron free path l.

(ii) If there is crystalline asymmetry in Δ_0 for In, it is less than $0.1kT_c$. The same conclusion was also arrived at by method I.

(iii) Methods I and II yield the same value, $(1.85 \pm 0.05)kT_c$, for Δ_0 for the 0.09-at.%-Sn specimens. However, as we proceed from 0.09-at.% Sn to lower concentrations and to pure In, the Δ_0's derived by methods I and II differ, and the difference grows progressively larger as pure In is approached. As the difference in Δ_0's by the two methods increases, the departure of the $\Delta(T)$-vs-T curve from the BCS relation Eq. (2) grows.

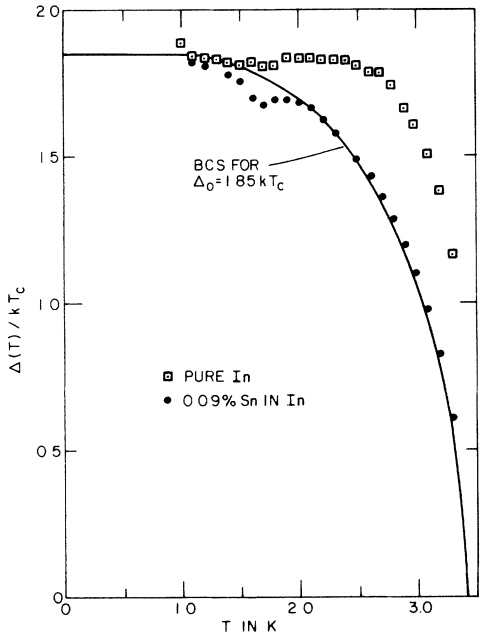

FIG. 3. Comparison of $\Delta(T)/kT_c$ for pure In and for the 0.09-at.% alloy with the theoretical BCS curve [Eq. (2)] for $\Delta_0/kT_c = 1.85$ and $T_c = 3.4\,0$ K. The pure-In and alloy data points were calculated by method II using Eq. (1) and the experimental $\alpha_s'(T)$, $\alpha_n'(T)$ data. $\vec{q}$ was in the [110] direction for both specimens.

This is demonstrated in Fig. 3. Table II shows also, that as we proceed from 0.09-at.% to lower concentrations of Sn, the ratio $\alpha_n(0)\,(\text{calc})/\alpha_n'(0)$ (expt) progressively decreases.

(iv) $\Delta(T)$ calculated from the precise measurements of H_c for pure In by Finnemore and Mapother[5] agrees with the BCS relation [Eq. (2)] with $\Delta_0 = 1.83kT_c$. We believe that $\Delta(T)$ for In agrees with the BCS relation and that Eqs. (1) and (2) characterize the attenuation of longitudinal ultrasound that results from the direct interaction of conduction electrons with the sonic beam. We attribute the departures from the BCS relation [Eq. (2)] of our $\Delta(T)$'s, calculated with Eq. (1), to a component of the sonic attenuation in our specimens that (i) is not described by Eq. (1), (ii) is different in the normal and superconducting states, and (iii) is temperature dependent. That this added attenuation is different in the normal and superconducting states is evidence that the conduction electrons must be involved in the attenuation process, but this cannot be the result of direct interaction of conduction electrons with the sonic beam because that kind of attenuation fits Eqs. (1) and (2). Mason[1] has proposed a theory for a kind of attenuation indirectly by the conduction electrons that fits the requirements. It is sonic absorption by line dislocations (crystal imperfections) whose vibrations between pinning points of the dislocation lines are damped by the conduction electrons in the normal state of the metal and by the quasiparticle excitations in the superconducting state.

IV. DISLOCATION DAMPING

In this section it is demonstrated that our experimental $\alpha_s'(T)$, $\alpha_n'(T)$ data for pure In and the three alloys with Sn can be consistently interpreted as resulting from a combination of (i) direct attenuation of the sonic beam by conduction electrons that satisfies BCS Eqs. (1) and (2) with $\Delta_0 = 1.85kT_c$, and (ii) attenuation of the sonic beam by vibrations of line dislocations that are forced to vibrate by the sonic beam and are damped by the conduction electrons. The vibrations are transverse to the dislocation line and take place in a crystalline glide plane.

The energy of vibration of dislocations may be dissipated in two ways of interest to us. If the sonic amplitude is small, the dislocations also vibrate with small amplitude, bowing out between adjacent pinning points for the dislocations for which pinning points act as nodal points for the vibration. Impurity atoms act as pinning points and the attenuation is independent of the sonic amplitude. When the sonic amplitude and the amplitude of the dislocation vibrations are large, dislocations break away from their pinning points and continue to vibrate in a smaller number of line segments of longer length and greater amplitude. The breaking of dislocation lines from pinning points involves the absorption of additional energy from the sonic beam in order to overcome the pinning forces and increase the vibration amplitude. The breaking of the pinning points makes the attenuation coefficient for the sonic beam dependent upon the amplitude of the sonic beam.

Attenuation by dislocations that is dependent on the sonic amplitude has been more extensively observed and studied than attenuation by dislocations that is amplitude independent. We are concerned here with attenuation that is independent of the sonic amplitude. Experimental evidence has been given in Sec. II proving that the attenuation we observed was independent of the sonic amplitude.

A differential equation[1] for small amplitude vibrations of a dislocation segment between pinning points, usually provided by impurity atoms, is

$$\rho b^2\left(\frac{\partial^2 x}{\partial t^2}\right) + B\left(\frac{\partial x}{\partial t}\right) - \frac{\mu b^2}{2}\left(\frac{\partial^2 x}{\partial y^2}\right) = T_{13} b\,, \tag{5}$$

where x is the transverse displacement of a point on a dislocation line at a position y along the dis-

location segment between its two pinning points, b is the Burger's vector for the dislocation, μ is the shear modulus of the specimen material in the glide plane of the dislocation, ρ is the crystal density, and T_{13} is the shearing stress generated by the sonic beam. T_{13} is in the glide plane for the dislocation and has the same direction as the Burger's vector $\vec{b}$. B is a damping constant and $-B(\partial x/\partial t)$ is the damping force exerted by the conduction electrons per unit length of dislocation. ρb^2 is the mass per unit length of dislocation, $\frac{1}{2}\mu b^2$ is the dislocation line tension, and $T_{13}b$ is the force per unit length of dislocation segment driving the vibrations with the sonic frequency. For a shearing stress T_{13} that varies slowly in the glide plane, a solution of Eq. (5) for a loop-shaped displacement between pinning points of a dislocation line is $x = A(l_0 y - y^2)$, where l_0 is the length of the dislocation line between two pinning points.

Mason[1] has shown that the acoustic-attenuation coefficient for forced vibrations of dislocations with small amplitudes is

$$\alpha_d = \frac{Q^{-1}\omega}{2V_s} = \frac{\omega}{2V_s}\frac{\bar{N}Rl_0^2(\omega/\omega_0)}{6[1+(\omega/\omega_0)^2]} , \qquad (6)$$

where Q is the response parameter of the oscillator, V_s is the velocity of sound, $\omega_0 \equiv (6\mu b^2/Bl_0^2)$, $\bar{N} \equiv N_0 l_0$ is the total length of line dislocations per cm^3 of specimen, and R is an orientation factor that depends on the type and direction of propagation—it usually varies between 0.08 and 0.02. Mason[1] set $R = 0.10$ for In.

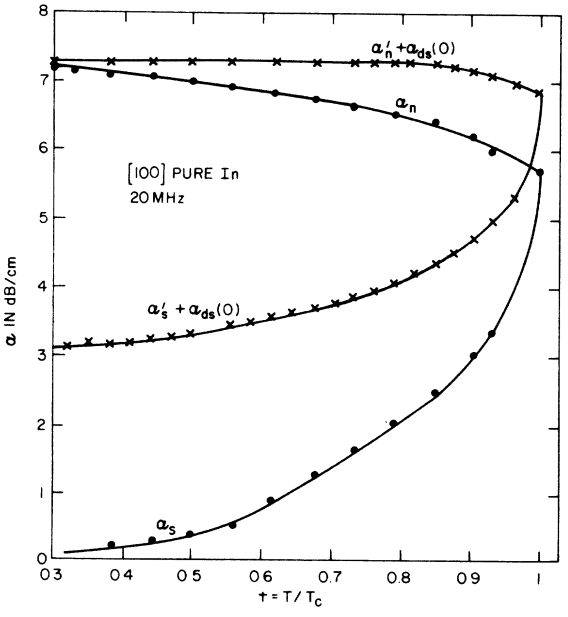

FIG. 4. Typical graph for a pure-In specimen, showing $\alpha_{dn}(T)$, $\alpha_{ds}(T)$, $\alpha_n(T)$, and $\alpha_s(T)$ deduced from the experimental $\alpha_s'(T)$, $\alpha_n'(T)$ data on the basis of (i) the Mason theory for dislocation attenuation and (ii) the BCS theory.

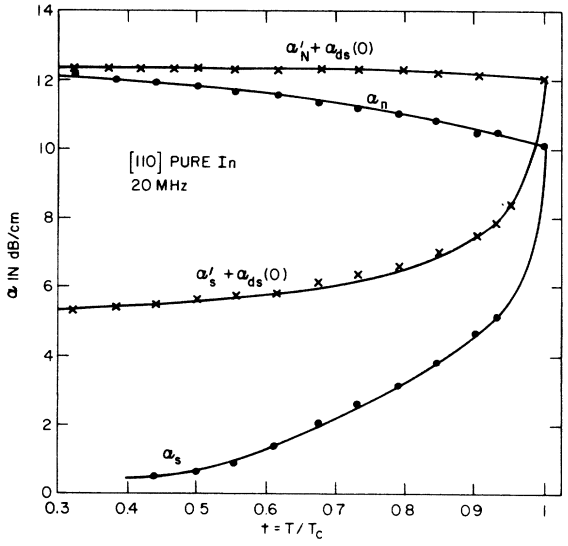

FIG. 5. Typical graph for a pure-In specimen, showing $\alpha_{dn}(T)$, $\alpha_{ds}(T)$, $\alpha_n(T)$, and $\alpha_s(T)$ deduced from experimental $\alpha_s'(T)$, $\alpha_n'(T)$ data on the basis of (i) Mason's theory for dislocation attenuation and (ii) the BCS theory.

The parameter B that characterizes the damping by conduction electrons of dislocation vibrations is proportional to the number density n of the conduction electrons and the electron mean free path l. The temperature dependence of B_n for the normal state and the relation of $B_n(T)$ to $B_s(T)$, for the normal and superconducting states, are determined by the dependence of nl on T and on the state, normal or superconducting. Conductance measurements on our specimens at liquid-He temperatures were not available for the determination of the temperature dependence of l. For very pure metals at liquid-He temperatures, $l \propto T^{-5}$, and for very impure metals and alloys, $l \propto T^0$. The best fit of our data with the Mason and BCS theories is obtained with $l \propto T^{-2}$. Hence, we have

$$\frac{B_n(T)}{B_n(T_c)} = \frac{\omega_{0n}(T_c)}{\omega_{0n}(T)} = \left(\frac{T_c}{T}\right)^2 \qquad (7)$$

and

$$\alpha_{dn}(T) = \alpha_{dn}(T_c)\frac{\omega_{0n}(T_c)}{\omega_{0n}(T)}\frac{1+[\omega/\omega_{0n}(T_c)]^2}{1+\omega/\omega_{0n}(T)} . \qquad (8)$$

These equations were used to calculate $\alpha_{dn}(T)$, the dislocation attenuation in the normal state (see Figs. 4 and 5), when $\alpha_{dn}(T_c)$ and $\omega_{0n}(T_c)$ were provided.

Because B for the normal state is proportional to the density of conduction electrons n and to the density of quasiparticle excitations, n_s in the super-

conducting state, we have

$$\frac{B_s(T)}{B_n(T)}=\frac{\omega_{0n}(T)}{\omega_{0s}(T)}=\frac{n_s}{n}=\frac{\alpha_s(T)}{\alpha_n(T)}=\frac{2}{1+e^{\Delta(T)/kT}} \tag{9}$$

and

$$\alpha_{ds}(T)=\alpha_{dn}(T)\,\frac{\omega_{0n}(T)}{\omega_{0s}(T)}\,\frac{1+[\omega/\omega_{0n}(T)]^2}{1+[\omega/\omega_{0s}(T)]^2}\,. \tag{10}$$

Equation (10) was used to calculate $\alpha_{ds}(T)$, the dislocation attenuation in the superconducting state, when $\alpha_{dn}(T)$ and $\omega_{0n}(T)$ were provided.

Equations (7)–(10) and

$$\alpha_s'(T)=\alpha_s(T)+\alpha_{ds}(T)-\alpha_{ds}(0)\,, \tag{11}$$

$$\alpha_n'(T)=\alpha_n(T)+\alpha_{dn}(T)-\alpha_{ds}(0) \tag{12}$$

were used to find, by trial and error, values for $\alpha_{dn}(T_c)$ and $\omega_{0n}(T_c)$ that yielded values for $\alpha_n(T)$ and $\alpha_s(T)$ that best satisfied the BCS Eqs. (1) and (2) with $\Delta_0=1.85kT_c$. The values adopted for the adjustable parameters were as follows: for the pure-In specimen with the [100] orientation, $\alpha_{dn}(T_c)=1.15$ dB/cm and $\omega_0=25\times10^6$ Hz; and for the pure-In specimen with the [110] orientation, $\alpha_{dn}(T_c)=1.92$ dB/cm and $\omega_0=25\times10^6$ Hz.

Figures 4 and 5 show the calculated values for $\alpha_{dn}(T)$ and $\alpha_{ds}(T)$ for pure-In specimens with $\vec{q}$ along the [100] and [110] directions. The deduced values of α_s and α_n for In without dislocation attenuation are also shown. Figures 6 and 7 compare $\Delta(T)/kT_c$ calculated using Eq. (1) from the derived $\alpha_n(T)$, $\alpha_s(T)$ data in Figs. 4 and 5 with $\Delta(T)/kT_c$ calculated from the experimental $\alpha_s'(T)$, $\alpha_n'(T)$ data.

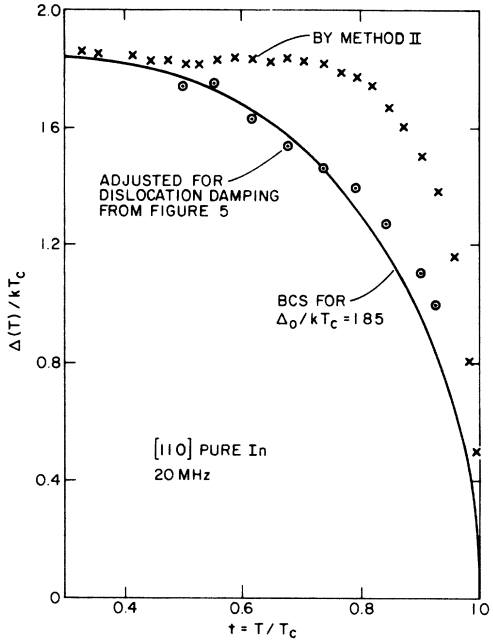

FIG. 7. Comparison of $\Delta(T)/kT_c$ determined by method II directly from the experimental $\alpha_s'(T)$, $\alpha_n'(T)$ data with $\Delta(T)/kT_c$ calculated by method II after adjustment for dislocation attenuation. Figure 7 was derived from data in Fig. 5.

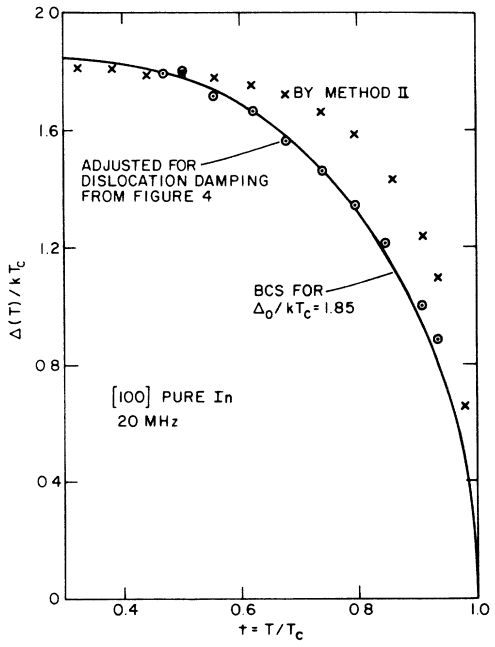

FIG. 6. Comparison of $\Delta(T)/kT_c$ determined by method II directly from the experimental $\alpha_s'(T)$, $\alpha_n'(T)$ data with $\Delta(T)/kT_c$ calculated by method II after adjustment for dislocation attenuation. Figure 6 was derived from the data in Fig. 4.

The experimental $\alpha_s'(T)$, $\alpha_n'(T)$ data for the 0.09-at.%-Sn alloy fit the BCS relations (1) and (2) very well with $\Delta_0=(1.85\pm0.07)kT_c$ when analyzed by either method I or II (see Fig. 3). Both methods yield essentially the same value for Δ_0 for the 0.09-at.% alloy, and this value agrees with the Finnemore and Mapother[4] value for pure In. From this it is concluded that sonic attenuation by dislocations in the 0.09-at.% alloy is negligible. This may be expected on the basis of Mason's theory since the solute Sn atoms make impurity center pinning points for line dislocations. As a consequence the length l_0 of the vibrating line segments are small; ω_0, which is proportional to l_0^{-2}, is large, and α_d is small. For the large ω_0's, α_d is proportional to l_0^4. For the 0.09-at.% alloy, α_d is so small that the observed $\alpha_s'(T)$, $\alpha_n'(T)$ data are practically equal to $\alpha_s(T)$, $\alpha_n(T)$.

For the 0.01- and 0.03-at.%-Sn alloy specimens, the departures of $\Delta(T)$ obtained with method II from the BCS curve for $\Delta_0=1.85kT_c$ decrease progressively as the Sn content is increased, from maximum departure for pure In to practically zero de-

parture at 0.09-at.% Sn. The dislocation attenuation α_d likewise decreases progressively from its maximum value for pure In to practically zero at 0.09-at.% Sn.

V. SUMMARY

The attenuation of ultrasound by dislocations that is dependent on the sonic amplitude has received more attention than dislocation attenuation that is independent of the sonic amplitude. There is an impression that the attenuation by dislocations that is independent of the sonic amplitude is negligible in comparison with the direct sonic attenuation by the conduction electrons. It is our belief that in the case of soft metals like In, the amplitude–independent attenuation by dislocations may be comparable with the direct attenuation of sound by the conduction electrons. We have demonstrated this for In.

The low values for Δ_0 in Table III can be explained by appreciable amplitude-independent dislocation attenuation. The agreement in Table III between different laboratories seems fortuitous as it would not be expected that acoustic specimens prepared in different laboratories by different investigators would have the same dislocation attenuation. Since our method II for handling the experimental data does not take account of dislocation attenuation, it seems fortuitous, also, that our extrapolation of the $\Delta(T)$'s for pure In to 0 K gave 1.85 for Δ_0/kT_c.

We find with our In specimen containing 0.09 -at.% Sn, as has been observed before for other soft metals, that an impure specimen ($l \lesssim \xi_0$) can give a better value for Δ_0 than a pure specimen.

---

*Work supported by the Applied Research Laboratory of The Pennsylvania State University under contract with the U. S. Naval Ordnance Systems Command.

[1]W. P. Mason, Phys. Rev. 143, 229 (1966); and *Physical Acoustics*, edited by W. P. Mason (Academic, New York, 1966), Vol. IV, Part A, Chap. 8.
[2]J. Bardeen, L. N. Cooper, and J. R. Schrieffer, Phys. Rev. 108, 1175 (1957).
[3]B. Mühlchlegel, Z. Phys. 155, 313 (1959).
[4]E. S. Bliss and J. A. Rayne, Phys. Rev. 177, 673 (1969).
[5]D. K. Finnemore and D. E. Mapother, Phys. Rev. 140 A 507 (1965).
[6]P. W. Anderson, J. Phys. Chem. Solids 11, 26 (1959).
[7]P. L. Richards and M. Tinkham, Phys. Rev. 119, 575 (1960).
[8]D. M. Ginsberg and M. Tinkham, Phys. Rev. 118, 990 (1960).
[9]J. D. Leslie and D. M. Ginsberg, Phys. Rev. 113, A362 (1964).
[10]I. Giaever and K. Megerle, Phys. Rev. 122, 1101 (1961).
[11]N. V. Zavaritskii, Zh. Eksp. Teor. Fiz. 43, 1123 (1962) [Sov. Phys.-JETP, 16, 793 (1962)].
[12]C. K. Campbell and D. G. Walmsley, Can. J. Phys. 45, 159 (1967).
[13]R. F. Averill, L. S. Strauss, and W. D. Gregory, Appl. Phys. Lett. 20, 55 (1972).
[14]H. R. O'Neal and N. E. Phillips, Phys. Rev. 137, A748 (1965).
[15]A. C. E. Sinclair, Proc. Phys. Soc. (London) 92, 962 (1967).
[16]K. Fossheim and J. R. Leibowitz, Phys. Lett. 22, 140 (1966).
[17]V. D. Fil, O. V. Shevchenko, and P. A. Bezuglyi, Zh. Eksp. Teor. Fiz. 52, 891 (1967) [Sov. Phys.-JETP 25, 587 (1967)].
[18]J. LePage, A. Bernalte, and D. A. Lindholm, Rev. Sci. Instr. 39, 1019 (1968).
[19]F. G. Brickwedde, H. van Dijk, J. R. Clement, and J. K. Logan, J. Res. Natl. Bur. Std. (U. S.) 64A, 1 (1960).
[20]R. W. Reed, D. E. Binnie, and F. G. Brickwedde, J. Acoust. Soc. Am. 51, 910 (1972).
[21]J. M. Perz, Can. J. Phys. 44, 1756 (1966).
[22]A. B. Pippard, Proc. Roy. Soc. (Lond.) A 257, 165 (1960); and *The Dynamics of Conduction Electrons* (Gordon and Breach, New York, 1965).